Chemical Engineering Journal 100 (2004) 23–32

Chemical Engineering Journal
www.elsevier.com/locate/cej

Catalytic combustion of methane in non-permselective membrane reactors with separate reactant feeds

Marcello Murru, Asterios Gavriilidis*

Department of Chemical Engineering, University College London, Torrington Place, WC1E 7JE London, UK

Received 30 July 2003; accepted 19 November 2003

Abstract

Catalytic combustion of methane over Pd and Pt/SiO_2/α-Al_2O_3 membranes was studied in the temperature range 300–650 °C. Fuel and oxygen were fed at opposite membrane sides. In order to improve reactor controllability the α-Al_2O_3 membranes were impregnated with SiO_2 sol resulting to smaller pore size. Methane conversions up to 100% for the palladium membrane and up to 42% for the platinum membrane were achieved. The results indicated a transition from kinetic to mass transfer control within the temperature range investigated. This was accompanied by reduction of methane slip from tube to shell side with increasing temperature. CO and H_2 were detected in the product gases of the palladium membrane. Their concentration could be reduced by applying a trans-membrane pressure difference. Low concentrations of CO were observed for the Pt/SiO_2/α-Al_2O_3 membrane, while no CO or H_2 were detected for a Pd/α-Al_2O_3 membrane operating in dead-end configuration.

Keywords: Catalytic membrane reactors; Pd; Pt; Methane; Combustion

1. Introduction

In recent years the popularity of ceramic membranes has constantly increased and such devices have found various applications especially in the fields of filtration and separation of gases and liquids. Research in ceramic catalytic membrane reactors has attracted considerable attention as testified by the large number of publications on the subject [2,14,15,19,31]. Although research in the field has mainly focused on multi-functional reactors, which combine simultaneous reaction and separation, membrane reactors have also been used for reactions taking place inside the pores of non-permselective membranes where reactants are fed to opposite membrane sides. This configuration provides flexibility for reactions normally requiring strict stoichiometric feed rates of reactants and inhibits reactant slip to opposing sides of membrane, provided reactions are sufficiently fast [22,23]. Separate feed of reactants offer advantages for hydrocarbon oxidation processes with respect to safety. When mixing of reactants is restricted by flammability considerations, premixing can altogether be avoided by such design. Furthermore, thermal runaway and consequently catalyst damage can be prevented since the reactor can operate under mass transfer control [28]. Finally, by applying a pressure difference over the membrane, products can be shifted preferentially towards the low pressure chamber keeping the hydrocarbon pure enough for recycling and increasing the overall conversion [20].

The aim of the present work is to study the performance of a membrane reactor with separate feed of fuel and oxygen in methane catalytic combustion in open-end and dead-end configurations. Technical difficulties related to the resistance of materials, as well as problems with stability of catalysts arise from the high temperatures involved. Experimental studies about catalytic combustion on membrane reactors have been carried out in [11,16–18,21] under isothermal conditions. One of the crucial and challenging problems faced in this investigation is the selection of suitable materials, especially for what concerns joining ceramic membranes to the stainless steel housing. Sealing of membrane reactors at high temperatures is an important and still largely unresolved issue [7,17].

Catalytic combustion is a demanding application in the field of catalysis, requiring thermally and chemically stable materials that have to guarantee steady operation for several hours [5,12,25,26,32]. In order to be competitive as combustors, catalytic systems have to meet the requirement of low emissions, stability and versatility under different regimes.

---

* Corresponding author. Tel.: +44-20-7679-3811;
fax: +44-20-7383-2348.
E-mail address: a.gavriilidis@ucl.ac.uk (A. Gavriilidis).

1385-8947/$ – see front matter © 2003 Elsevier B.V. All rights reserved.
doi:10.1016/j.cej.2003.11.015

Low catalyst stability has certainly been one of the main reasons for the limited use of catalytic combustion systems. Lean mixtures are usually employed in modern combustors since they can effectively reduce the amount of unburned fuels and NO_x. This fact has focused most investigations on these conditions while little is known about the behaviour of combustion of rich mixtures. It has been demonstrated that the use of lean mixtures in catalytic systems also reduces deactivation and instability of catalysts, prolonging life and providing steady performance of combustors [24].

In the present investigation, the combustible mixture composition varies from very rich to very lean within the porous catalyst phase. Accordingly, the catalyst can show different behaviour depending on the position along the membrane radius. It is important to note that, even if the catalytic membrane is uniform throughout the cross-section, different reaction mechanisms and catalyst transformations can take place in different positions. For this reason, two catalytic materials were investigated, palladium and platinum.

2. Experimental set-up

2.1. Catalytic membrane preparation

Initially, α-Al_2O_3 membrane supports (HITK, 7 cm i.d. and 10 cm o.d.) with 30% porosity and average pore size of 1.8 μm were used for the experiments. However, their high permeability made the reactor difficult to control when pressure disturbances occurred during open-end experiments. Permeability was decreased by depositing colloidal SiO_2 (Buehler Mastermet2) inside the membrane pores. Membranes were cut to size (10 cm), sonified in an ultrasonic bath with DECON90 (Fisher) and the surfaces of their bases polished with sand paper in order to make them flat and smooth. Overnight intrusion of the colloidal silica solution inside the pores of the support was followed by freeze drying and calcination at 800 °C. This procedure allowed uniform distribution of pore size throughout the cross-section. The resulting average pore size was ca. 0.4 μm, as determined by mercury porosimetry. The surface of the membrane was dried with adsorbing paper before freeze drying in order to reduce the possibility of formation of SiO_2 top layers. The palladium precursor was 5 wt.% Pd tetra-amine palladium nitrate solution $(NH_3)_4Pd(NO_3)_2$ (Johnson Mattey), with pH = 2.1. Chloroplatinic acid solution (pH = 1.21), obtained diluting $H_2PtCl_6 \cdot 6H_2O$ (99.95% purity, Alpha Aesar) with distilled water was used to prepare Pt membranes. Overnight impregnation for both Pt and Pd was followed by calcination at 600 °C for 2 h. XRD analysis for the palladium membrane indicated the presence of both Pd and PdO, the latter being more prominent after use. Loading of the palladium membrane used for the open-end experiments as measured by atomic adsorption, was 0.402 wt.% while that for Pt membrane was 0.17 wt.% Pt. For dead-end experiments, membrane modification with colloidal SiO_2 was not necessary since reactor performance is not affected by pressure disturbances and high permeability is beneficial. The membrane used for these experiments had 0.9 wt.% Pd loading. More information on support modification by colloidal silica and catalyst impregnation are given by Murru et al. [9].

2.2. Set-up configuration

Fig. 1 shows the experimental set-up used for the evaluation of the catalytic membrane performance. Nitrogen or helium were used to dilute methane that was fed in the tube side. The oxidising mixture, always fed in the shell side, was air or He + O_2. The latter mixture proved to be useful since it allows the GC (when using He as carrier gas) to detect oxygen without the interference of nitrogen peak in the chromatogram. Mass flow controllers (Brooks 5850TR) were used to supply gases to the tube and the shell side of the reactor.

Temperatures of inlet and outlet streams were continually monitored and recorded via a data acquisition terminal connected with type K thermocouples. The axial temperature profile of the tube side was examined using a thermocouple that could be shifted along the axis of the reactor. A differential manometer was connected to the two outlets of the reactor in order to continually monitor pressure difference across the membrane. Unless otherwise specified, all experiments were performed at atmospheric pressure.

Sealing was achieved either by radially compressing a graphite ribbon around the external surface of the membrane (radial sealing) as described by Lafarga et al. [7] or by axially compressing the flat surfaces of the membrane with Millboard (James Walker Ltd.). When the radial sealing was used, the two ends of the membrane were made impermeable by glazing with enamel (Cookson Matthey) in order to make the sealing leak-proof. An ultra-pure graphite tape (NGP G6103-GTJ nuclear grade graphite ribbon) was used to create the seal between tube and shell side. The reactor was considered sealed when, after pressurising at 5 bar no leaks could be detected. This method of sealing was reliable up to 480–500 °C but the graphite layer was burnt after a couple of days at 530 °C.

For high temperature operation the axial sealing was used. As shown in Fig. 2, the inlet tube is a thick stainless steel stem that can slide in the inlet section and is pushed by a spring towards the membrane. The axial sealing system is divided in two parts. The first part provides a sealing between the reactor shell and the membrane and between the stem and the membrane. A ceramic flexible material (Millboard by James Walker Ltd.) was placed between the membrane bases and the metal surfaces. The second part of the system is located outside the reactor area and is made up of two viton o-rings fixed into two grooves in the movable stem of the inlet tube. This way leaks are avoided between the stem and its stainless steel guide. A spring is used to push the stem while absorbing the stress on the membrane caused by the thermal expansion of the materials upon heating or

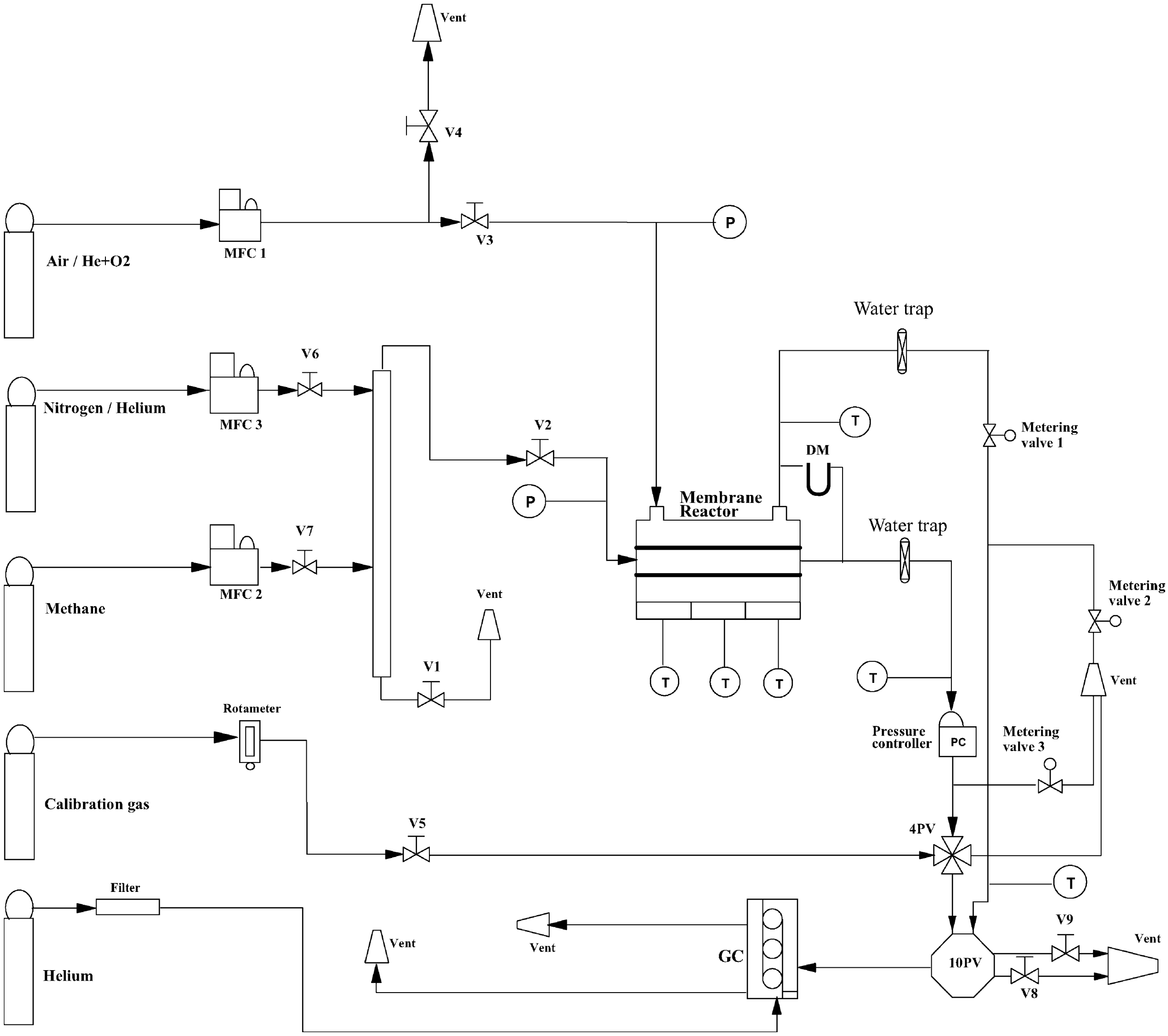

Fig. 1. Experimental set-up. MFC: mass flow controller, V: toggle valve, 4PV: four way valve, 10PV: 10-port valve, DM: differential manometer, T: thermocouple, P: pressure gauge, GC: gas chromatograph.

cooling the reactor body. The reactor shell is in turn sealed with two flanges using copper gaskets. Since the stem has a rather thick wall (about 5 mm), axial heat conduction can heat up the viton o-rings therefore a simple tube-shell heat exchanger was fitted onto the external surface of the inlet section in order to prevent damaging them. This system was able to withstand temperatures as high as 700 °C but it is likely to cope at higher temperatures since the Millboard is

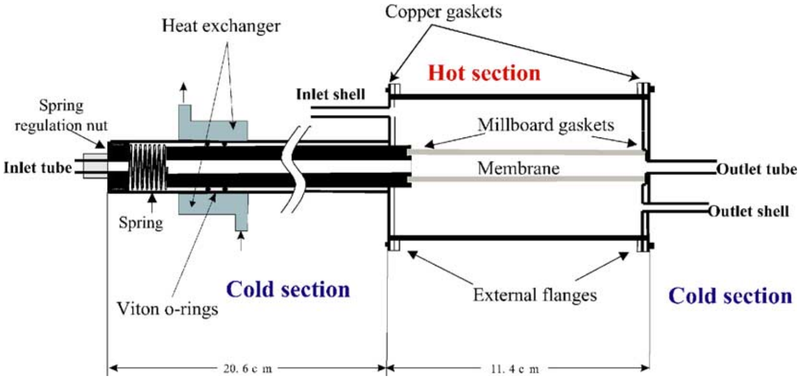

Fig. 2. Reactor axial sealing.

certified for at least 800 °C. Up to a pressure of 3 bar no leaks from tube to shell side and no leaks outside the reactor were detected.

Depending on the flow pattern of the gases in the membrane reactor two different configurations were used, namely open-end and dead-end. Open-end configuration implies that the reactor has two inlets and two outlets, one for each channel. Radial diffusion is the main transport mechanism through the porous membrane and the convective fluxes inside the channels have parallel directions (axial). When one of the two outlets is plugged a dead-end configuration is obtained. Gas from the plugged channel permeates through the membrane mainly by convection, and counter diffusion of other species takes place from the opposite side towards the membrane. When the reactor is operated in a dead-end configuration, the membrane is not only the catalyst support but it also behaves as a gas distributor [1]. In all the dead-end experiments, methane was the reactant chosen to permeate through the membrane because of its lower flowrate.

For the open-end experiments 10 cm SiO_2/Al_2O_3 membranes, impregnated with Pd and Pt (not enamelled) were used in the axial sealing reactor configuration (28 mm i.d.). A mixture of 20.5 vol.% O_2 in He (BOC) was fed to the shell side at a flowrate of 200 ml/min while a mixture of CH_4 (BOC CP grade) in He (BOC CP grade) was fed to the tube side at 90 ml/min. The pressure inside the reactor and the pressure difference between the two channels were continuously monitored with a pressure gauge and a differential manometer. A pressure controller was used to keep the pressure of the tube side constant whereas a fine needle valve was used to keep the pressure difference between the tube and the shell side at the desired value. This control method proved to be reliable up to 3 mm of H_2O pressure difference. Due to difficulties in controlling the temperature inside the reactor, the latter was operated at constant heat input mode. For the axial sealing configuration, heat was provided only in the hot section of the reactor (see Fig. 2). Only its central area was heated whereas the inlet section had to be cold in order not to damage the two viton o-rings. Therefore inlet temperature at the location of the o-rings was about 60 °C. Two semi-cylindrical ceramic fibre heaters were used (Watlow). Each heater had a total length of 241 mm with an inner diameter of 89 mm and maximum power loading of 2.1 W/cm^2 at 60 V. In order to supply constant power at the heating elements careful control of the voltage in the range 78–95 V by a variac was employed. A voltmeter was connected to the electricity supply and the voltage of the power supply was continuously monitored so that suitable corrections to the variac were made. Temperature profiles of tube and shell side were always similar and were typically parallel with 10–15 °C difference.

In dead-end experiments the radial sealing reactor (30 mm i.d.) was always employed. The 10 cm membranes were used with approximately 1 cm occupied by the enamel/graphite sealing. The temperatures of the dead-end experiments could never exceed 500 °C because of the sealing limitation. Flowrate of air in the shell side was 180 ml/min and the flowrate of pure CH_4 fed in the tube was 10 ml/min. The reactor was placed in the middle of a furnace (Carbolite CST 10/75) and this allowed an isothermal temperature profile. Inlet and outlet tubes were within the radiation area of the heating elements, therefore the gases were fed already preheated.

For gas analysis a GC (Shimadzu GC-14B), equipped with a TCD detector was used. A 10-port sampling valve (VICI Valco) allowed alternate injections from two different sampling loops. Temperature of the TCD was 200 °C for all analyses at a carrier flowrate of 15 ml/min (He) and 20 ml/min (N_2). For dead-end experiments where N_2 was used as the inert gas a Carboxen-1000 15 ft × 1/8 in. SS (Supelco) with He as carrier gas was employed for separation of N_2, O_2, CO (at 50 °C), CO_2 and CH_4 (at 180 °C). For the open-end experiments where He was used as the inert gas, a Porapak Q 80–100, 60 m × 1/8 in. × 2 mm SS (Chrompack) was employed. He (BOC CP grade) was used as a carrier gas to separate O_2, CO, CH_4 and CO_2 at 200 °C while N_2 was employed as carrier gas to quantify H_2 at 35 °C. Both columns showed unreliable results when water was present in the gas mixture. In order to avoid the presence of water in the column, a water trap packed with calcium chloride (Fluka 1–3 mm particle size) was placed in the reactor outlets.

Since the gas analysis was on the dry streams, appropriate corrections were applied to the GC measured compositions in order to quantify component concentrations at the reactor outlets. The correction was calculated according to the following:

$$X_i = \frac{X_i'}{1 + 2X_{CO_2}'} \qquad (1)$$

where X_i and X_i' are the molar fractions of the generic component i at the outlet of the reactor and measured by the GC, respectively. Carbon balance closed within 3% for isobaric and within 7% for non-isobaric experiments. During every experimental run, at least three injections per stream were performed for each data point. In order to verify that a steady state had been reached, the temperature had to be stable and the measured molar fractions had to be equal in two consecutive analyses. Calibration was checked weekly using BOC certified calibration gases.

3. Membrane reactor experiments

Several experiments were carried out in order to assess the performance under different conditions and to determine the key factors that can affect operability. The possibility of catalyst deactivation during the course of the experimental work was assessed by carrying out twice the same experiments with the same Pd/SiO_2–Al_2O_3 membrane 3 months apart. Conversions decreased from 28 to 25.1% at 0.129 methane molar fraction and from 32.1 to 26.6% at 0.285

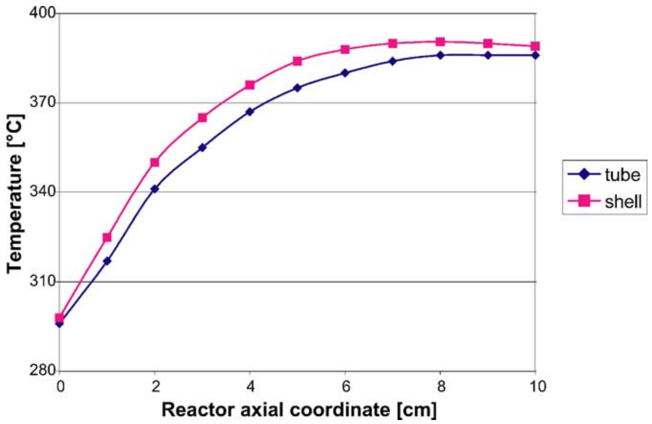

Fig. 3. Tube and shell side temperature profiles for membrane reactor when the voltage applied to the heaters was 78 V and the overall methane molar fraction 0.2. Temperature recorded during a reaction run. $Pd/SiO_2–Al_2O_3$ membrane reactor in open-end configuration.

methane mole fraction. This catalyst activity decrease was deemed to be acceptable for the purpose of this study.

3.1. Behaviour of $Pd/SiO_2–Al_2O_3$ membranes in open-end configuration

A blank run with a non-impregnated membrane was carried out in an open-end configuration. At 650 °C and 2% overall methane inlet concentration the conversion was zero and no combustion products were detected. Preliminary experiments showed that the fresh catalyst was not sufficiently stable and did not behave in a reproducible way. However, after few days operating at 78 V (average reactor temperature 365 °C) and 0.1 methane inlet molar fraction the performance of the reactor became stable.

Fig. 3 shows the temperature profile of the membrane reactor operating at 78 V. Reactor temperature varied from ca. 295 to 380 °C between inlet and outlet. Maximum temperature difference between tube and shell side was 10 °C. The same pattern of temperature profiles was observed at all other operating voltages. Temperature increases along the reactor main axis by the combined effects of heat being produced by the reaction and heat supplied by the heaters. The performance of the reactor was assessed under different conditions evaluating overall methane conversion (Eq. (2)), CO overall output concentration and methane slip from tube to shell side

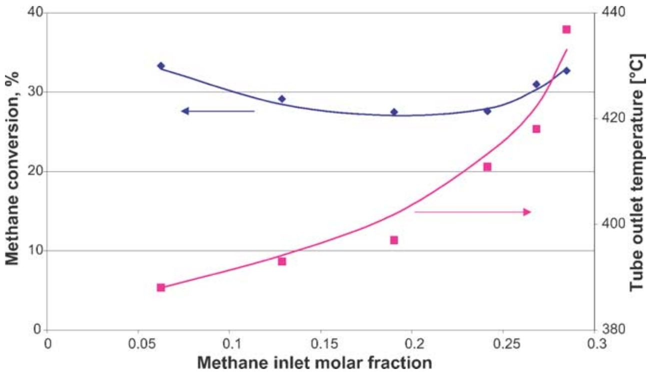

Fig. 4. Methane conversion and outlet temperature at tube side as a function of overall methane inlet molar fraction. Voltage applied to heaters 78 V. $Pd/SiO_2–Al_2O_3$ membrane reactor in open-end configuration.

$$\text{overall methane conversion} = \frac{\text{production rate of CO and CO}_2\ (\text{mol/s})}{\text{methane feed rate (mol/s)}} \tag{2}$$

3.1.1. Effect of heat supplied and inlet methane concentration

Four sets of experiments were performed in absence of trans-membrane pressure difference varying the voltages applied to the heaters. As shown in Figs. 4–7 conversion of methane is proportional to the voltage applied, since higher voltages always result to higher reactor temperatures while the tube outlet temperature is dependent on methane inlet molar fraction. The rate of methane combusted, and therefore the rate of heat produced is function of the amount of

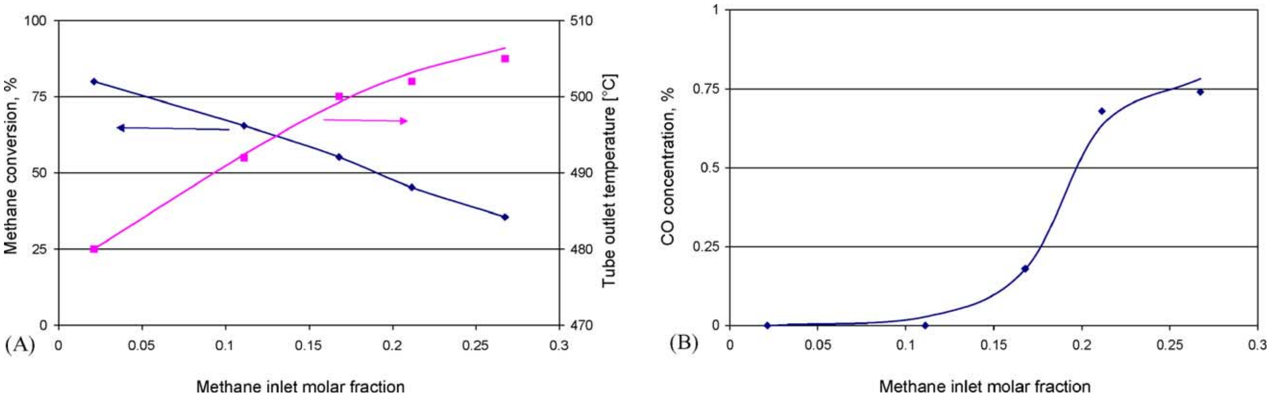

Fig. 5. (A) Methane conversion and outlet temperature at tube side, and (B) outlet CO concentration as a function of overall methane inlet molar fraction. Voltage applied to heaters 85 V. $Pd/SiO_2–Al_2O_3$ membrane reactor in open-end configuration.

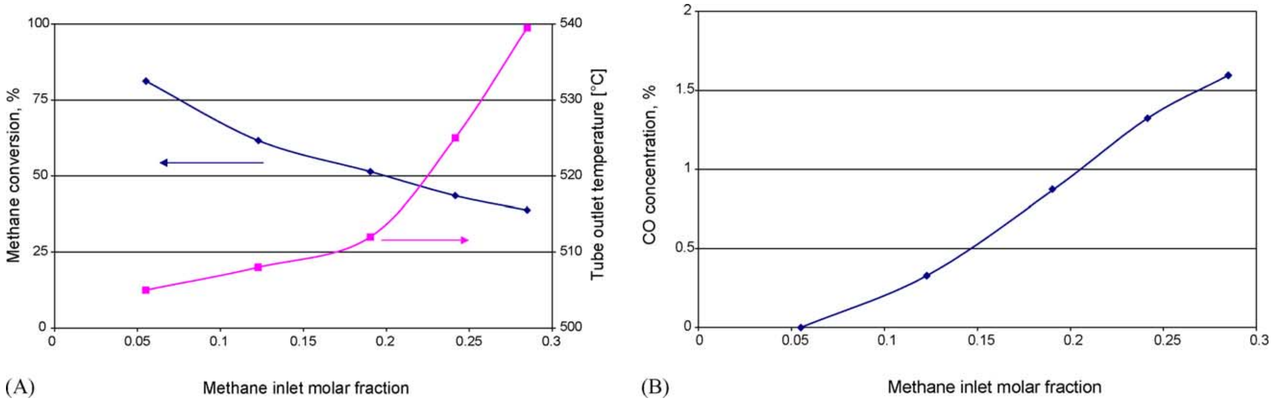

Fig. 6. (A) Methane conversion and outlet temperature at tube side, and (B) outlet CO concentration as a function of overall methane inlet molar fraction. Voltage applied to heaters 90 V. Pd/SiO_2–Al_2O_3 membrane reactor in open-end configuration.

methane in the feed. Accordingly, an increase of methane inlet concentration results to an increase of outlet temperature. Fig. 4 shows an increase of about 50 °C at the outlet temperature from the lowest to the highest molar fraction employed in the experiment which is higher than the other experiments at higher voltages as shown in Figs. 5–7 (25 °C at 85 V, 35 °C at 90 V, 45.4 °C at 96 V).

When increasing methane inlet concentration, conversion decreases for all experiments, except at 78 V where a minimum is observed at methane inlet mole fraction of 0.19. This minimum and the trend of conversion with methane mole fraction at various voltages can be explained if a transition from kinetic to diffusive control is postulated at ca. 430–480 °C. Since the order of methane catalytic combustion with respect to methane is in the range 0.5–0.8 [8,10,30], the increase of methane mole fraction is expected to increase reaction rate but decrease conversion (at isothermal conditions). This increase in reaction rate would result to an increase in temperature as observed in Fig. 4. However, under the assumption of kinetic control below 430 °C, the increase of temperature would result to an exponential increase of reaction rate and hence this would more than compensate the conversion decrease due to higher methane mole fraction. Figs. 5–7 would then represent operation under diffusive control. Even though mass transfer is a first order process, conversion decreases with methane mole fraction due to the shift of reaction zone inside the membrane towards the shell side. As can be concluded from Figs. 5–7, reaction rate increases with methane mole fraction, leading to a temperature increase. Under the assumption of diffusive control above 480 °C, the increase of temperature would result to a weaker increase of reaction rate which cannot compensate conversion decrease, resulting to a continuous decrease of conversion for the whole methane mole fraction range studied.

The runs at 78 V did not show any CO in the products even at higher methane inlet molar fractions. This is different from all other experiments at higher voltage (see Figs. 5B–7B) where higher temperatures cause more CO to be produced. Increase of CO concentration is also observed at higher methane inlet mole fractions.

CO was always present only in the tube side and it was never detected in the shell. It is produced mainly in the part of the membrane where the ratio CH_4/O_2 is high (closer to the tube side) and more easily diffuses to the bulk. Traces of CO might be present in the shell side since the detection limit of such gas is about 0.05% with the GC used in our

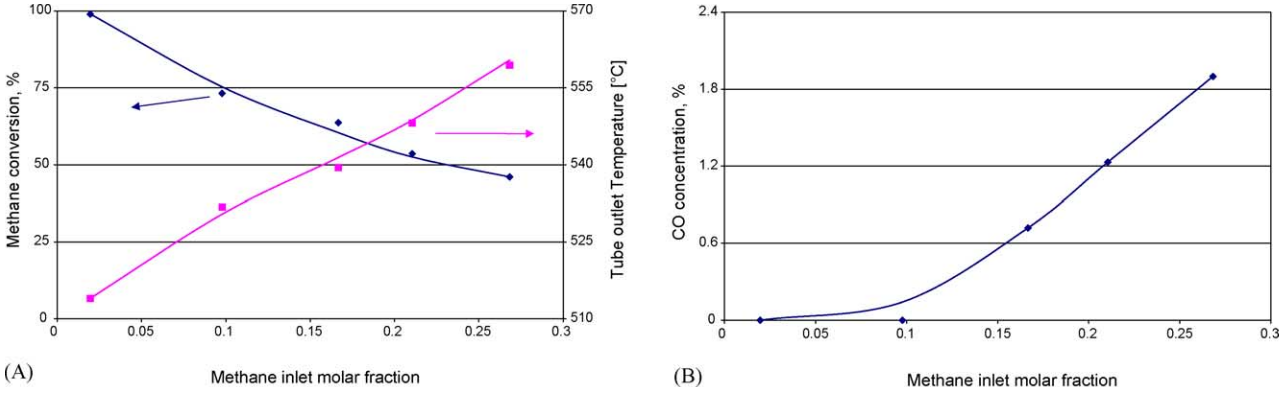

Fig. 7. (A) Methane conversion and outlet temperature at tube side, and (B) outlet CO concentration as a function of overall methane inlet molar fraction. Voltage applied to heaters 96 V. Pd/SiO_2–Al_2O_3 membrane reactor in open-end configuration.

experiments. H_2 was detected in almost all the experiments in absence of pressure gradients when CO was detected but it could not be quantified because He was used as carrier of the GC in isobaric runs. This behaviour is consistent with the fact that combustion of rich methane/air mixtures on palladium and platinum catalysts is accompanied by side reactions that produce CO and H_2. These include partial oxidations, steam reforming, reverse methanation and water gas shift [8,27,29]

$$CH_4 + \tfrac{1}{2}O_2 \rightleftharpoons CO + 2H_2 \quad (3)$$

$$CH_4 + \tfrac{3}{2}O_2 \rightleftharpoons CO + 2H_2O \quad (4)$$

$$CH_4 + H_2O \rightleftharpoons CO + 3H_2 \quad (5)$$

$$CH_4 + 2H_2O \rightleftharpoons CO_2 + 4H_2 \quad (6)$$

$$CO + H_2O \rightleftharpoons CO_2 + H_2 \quad (7)$$

Dry methane reforming according to reaction (8) is also possible:

$$CH_4 + CO_2 \rightleftharpoons 2CO + H_2 \quad (8)$$

Direct decomposition (reaction (9)) is unlikely to occur in the membrane reactor since very high temperatures (>750 °C) and very low residence time are required for it [27]

$$CH_4 \rightleftharpoons C + 2H_2 \quad (9)$$

Both palladium and platinum can promote partial oxidation and steam reforming [13]. Kikuchi and Chen [6] argue that partial oxidation results from an initial reaction of complete combustion which consumes all the oxygen. Then the produced water vapour and carbon dioxide reduce the residual methane to hydrogen. Something similar may occur also in the configuration studied in this work especially if we consider that excess CH_4 exists in the part of the membrane close to the tube side. According to this, CO and H_2 would be produced by dry and steam reforming reactions. However, contributions of the other reactions to CO and H_2 production cannot be excluded.

If the rate of reaction is not fast enough, methane and oxygen can slip through the membrane into the opposite channel. The slip of reactant can indicate whether the reactor is operating under mass transfer or kinetic control regime. If, for instance we suppose that the reaction is infinitely fast, all the reactant gases entering on one side of the membrane are completely consumed in an infinitely small area inside the membrane. This is the limiting case of mass transfer controlled reaction that clearly implies zero slip of both reactants. If one of the two reactants reaches at some point 100% conversion there is slip of the opposite reactant since the latter has no possibility of reacting inside the membrane. Fig. 8 shows the slip of methane for inlet methane molar fraction of 0.122 and a CH_4/O_2 ratio in the feed of 0.27 at different voltages applied to the heaters. Slip of methane at 78 V is more than two-fold the ones at higher voltages, which is consistent with the previous postulate of a transition from kinetic control towards mass transfer control.

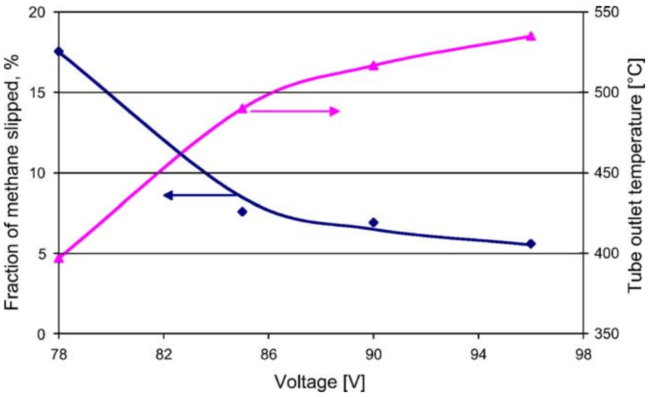

Fig. 8. Fraction of methane fed to the reactor that slips from tube to shell side and corresponding tube side outlet temperatures as a function of voltage applied to the heaters for inlet methane molar fraction of 0.122. $Pd/SiO_2–Al_2O_3$ membrane reactor in open-end configuration.

3.1.2. *Effect of trans-membrane pressure gradients*

One of the parameters that can affect the performance of a membrane reactor is the pressure difference applied across the membrane. The possibility of having a convective contribution to the radial fluxes of reactants and products makes membrane reactors potentially more versatile than ordinary monolithic reactors for catalytic combustion. Voltage applied to the heaters was 90 V and Table 1 shows the operating conditions of the non-isobaric experiments. Outlet temperatures of the tube side were in the range 520 ± 10 °C and the inlet was 100 °C lower than the outlet. Positive pressure differences correspond to higher shell side pressures. Permeation rates increased linearly with pressure difference and they reached 50 ml/min at 140 mbar. As shown in Fig. 9, conversion increased slightly from 47 to 50% in the range of ΔP from 0 to 140 mbar. Neomagus et al. [11] observed during methane combustion on platinum membrane reactor (see Table 1 for more details) similar small increase of methane conversion for an equivalent pressure drop. Saracco et al. [17] showed that the conversion of propane can increase by

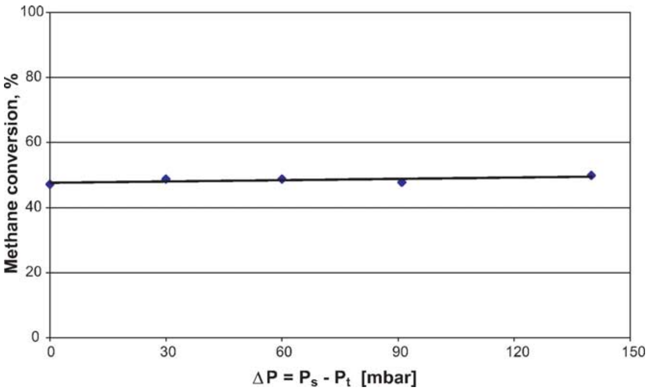

Fig. 9. Methane conversion with trans-membrane pressure gradients applied; 90 V were applied to the heaters and overall inlet methane molar fraction was 0.22. $Pd/SiO_2–Al_2O_3$ membrane reactor in open-end configuration.

Table 1
Experimental conditions of the present work and the ones by Saracco et al. [17] and Neomagus et al. [11] used for non-isobaric experiments

	Saracco et al. [17]	Neomagus et al. [11]	This work
Membrane internal radius (mm)	7	7	3.5
Membrane external radius (mm)	10	10	5
Shell radius (mm)	25	25	14
Catalyst	Platinum	Platinum	Palladium
Catalyst loading (wt.%)	1[a]	1, 7[a]	0.4
Average pore size (μm)	0.35	0.35	0.4
Porosity (%)	34.6	34.6–35.4	20
Hydrocarbon combusted	Propane	Methane	Methane
Hydrocarbon feed molar (%)	4 and 7	10	22
Tube side flowrate ($\mathrm{N\,m^3/s}$)	3.33×10^{-5}	15×10^{-6}	1.5×10^{-6}
Shell side flowrate ($\mathrm{N\,m^3/s}$)	3.33×10^{-5}	32×10^{-6}	3.33×10^{-6}
$P_{\mathrm{shell}}-P_{\mathrm{tube}}$ range (mbar)	$-2000 \Rightarrow 2000$	$0 \Rightarrow 1000$	$0 \Rightarrow 140$

[a] Catalyst loading refers to the weight of deposited γ-Al_2O_3 which, in turn has a loading of 4 wt.%.

up to 300% when a pressure difference of 1800 mbar is applied. They attributed this behaviour to the shifting of the reaction zone towards the low pressure side where the concentration gradients of the species moving against convective flow become steeper allowing higher diffusive fluxes and consequently higher conversion. The qualitative agreement between these three studies is satisfactory. Quantitative disagreement particularly between this work and Saracco et al. [17] is attributed to different experimental conditions used (see Table 1). It is worth noting that the thickness of membranes used by Saracco et al. [17] and Neomagus et al. [11] was twice the thickness of those used in this work, therefore higher convective fluxes were allowed by our membranes for same pressure difference.

Even though trans-membrane pressure difference was not found to be beneficial for conversion increase, it proved to be useful for reduction of CO and H_2 concentrations as shown in Fig. 10. This behaviour suggests that higher pressure difference promotes complete oxidation of methane as opposed to partial oxidation, steam reforming and water gas shift reactions. Since the mixture of helium and oxygen is pushed through the membrane from the shell towards the tube side, higher oxygen concentrations can be expected inside the membrane at higher pressure differences. A lower production of CO and H_2 could be due to a reduction of the oxygen deficient and water containing part of the membrane and hence areas where the above side reactions would take place. The higher amount of O_2 present could also promote oxidation of CO and H_2. Since H_2 is more reactive than CO, its concentration would decrease faster with ΔP as indeed is observed in Fig. 10. Alternatively, the faster concentration decrease of hydrogen may be due to different reaction steps through which CO and H_2 are formed in catalytic steam reforming [13].

3.2. Behaviour of Pt/SiO_2–Al_2O_3 membranes in open-end configuration

Isobaric experiments were carried out using the reactor with axial sealing in which the platinum impregnated membrane was mounted. CO was not present in the outlet gases even at high temperature (973 K) and good controllability of the reactor was observed. Despite high methane inlet concentrations, membranes impregnated with platinum yielded reproducible results and the catalyst did not need aging to achieve stable activity.

The feed of the tube side had a methane molar fraction of 22% (balance He) while 20.5% O_2 (balance He) was fed

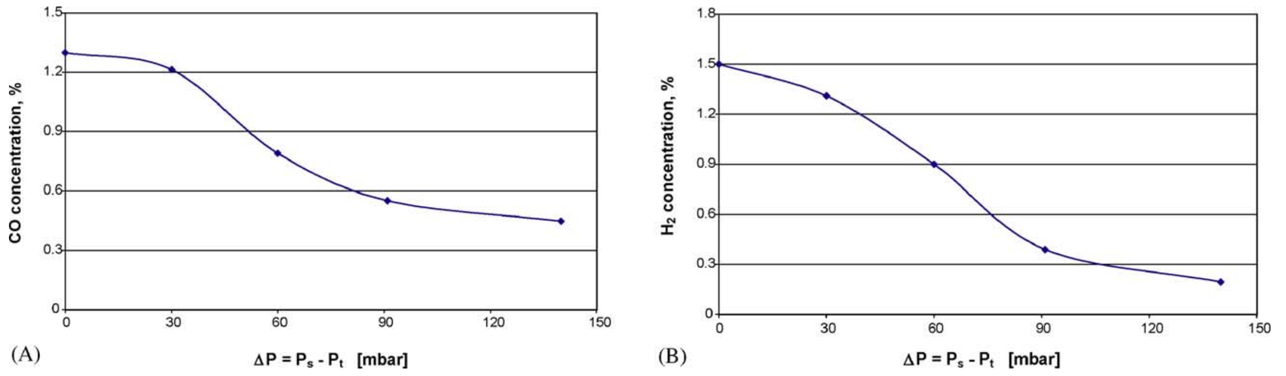

Fig. 10. CO (A) and H_2 (B) production as a function of the pressure difference applied across the membrane; 90 V were applied to the heaters and overall inlet methane molar fraction was 0.22. Pd/SiO_2–Al_2O_3 membrane reactor in open-end configuration.

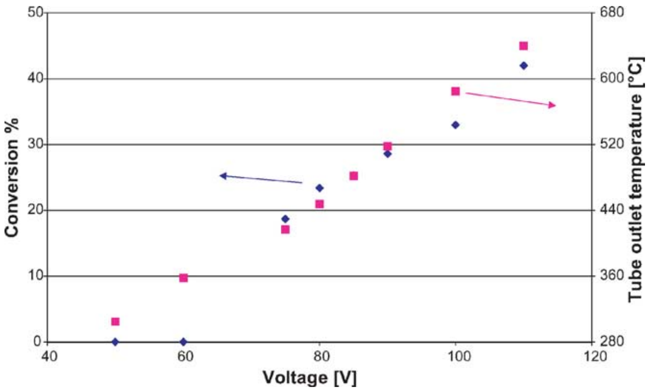

Fig. 11. Methane conversion and tube outlet temperature as a function of voltage applied to heaters. Overall methane inlet molar fraction 0.22. $Pt/SiO_2–Al_2O_3$ membrane reactor in open-end configuration.

to the shell side. Fig. 11 shows that reaction takes place if the voltage applied to the heaters is higher than about 60 V, which corresponds to outlet temperatures higher than 360 °C. Almost linear dependency of conversion and temperature with voltage is observed. Conversions achieved with Pt membranes are lower than the ones achieved with Pd membranes. This is due to the fact that Pd is more active than Pt in methane oxidation (cf. [3]), and its loading is higher in the catalytic membrane. Slip of methane from tube to shell side (Fig. 12) decreases when the heat supplied to the reactor is increased. The values of methane slip are in good agreement with the work by Neomagus et al. [11] who studied a similar system for methane combustion. However, conversions achieved in this work are slightly lower possibly because of lower catalyst activity. If one compares methane slip with the $Pd/SiO_2–Al_2O_3$ membrane, it is observed that for the latter this is lower due to higher Pd catalyst activity.

CO was detected only for temperatures higher than about 580 °C and in very low concentrations. The CO concentration in the tube side was 0.15% at 110 V (640 °C) and less than 0.1% at 100 V (585 °C). Carbon monoxide was not detected in the outlet gas of the shell side. Another difference with the experiments on Pd membranes is that H_2 was not detected even when CO was present in the outlet gas. The mechanism of CO and H_2 production on platinum may therefore be different from that on palladium. The activities of Pd and Pt for methane steam reforming are similar [13], and hence this behaviour can be related to lower water concentrations in the Pt membrane, since the latter is less active for combustion. Trimm and Lam [24] reported the production of CO for rich combustion of methane on Pt/Al_2O_3 catalysts at temperatures higher than 530 °C. Besides, deposition of carbon on the catalyst and consequent deactivation was observed. No deactivation was observed in our work.

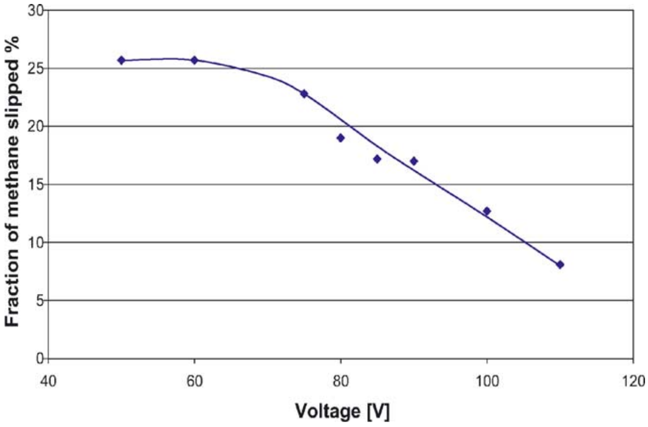

Fig. 12. Fraction of methane fed to the reactor that slips from tube to shell side as a function of voltage applied to heaters. Overall methane inlet molar fraction 0.22. $Pt/SiO_2–Al_2O_3$ membrane reactor in open-end configuration.

3.3. *Behaviour of Pd/Al_2O_3 membranes in dead-end configuration*

Non-modified α-Al_2O_3 membranes were used for dead-end experiments where the tube side outlet was plugged. The bare α-Al_2O_3 support was tested at 500 °C showing complete inactivity towards methane combustion. For these experiments the catalyst took 6–10 h to stabilise. Fig. 13 illustrates the dependence of conversion on inlet temperature of the shell side. Conversion versus temperature shows an S-shaped curve demonstrating ignition at around 350 °C, which is comparable with light off temperatures of catalytic monoliths for methane combustion [4]. Carbon monoxide and hydrogen were not detected in the dead-end experiments although the molar fraction of methane inside the membrane is very high especially next to the tube side. Effective diffusivity in non-modified membranes is higher because the porosity and pore diameter is larger. Accordingly, oxygen can diffuse effectively inside the membrane. Furthermore, convective flow of methane is relatively low (methane/air flowrates 10/180). The efficient contact of methane and oxygen inside the pores together with the lower operating temperatures can possibly be the causes of lower CO and H_2 concentrations observed. Furthermore, this may

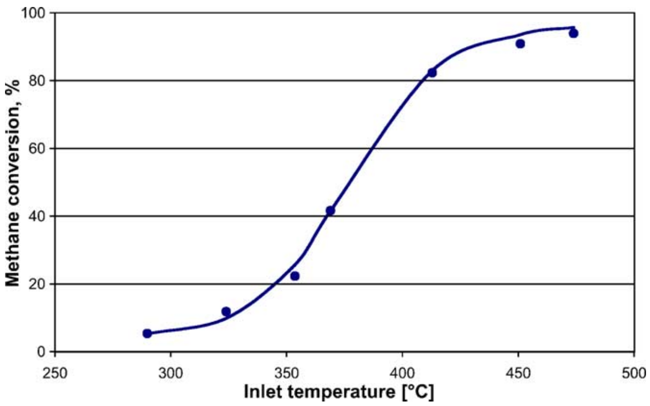

Fig. 13. Effect of inlet temperature on methane conversion. Pd/Al_2O_3 membrane in dead-end configuration.

also be due to the absence of silica in the membrane, since the support is probably involved in the reforming reaction by influencing the activation of steam [13].

4. Conclusions

A novel membrane reactor was designed and built that can operate at high temperatures and a new sealing concept was successfully developed. Methane and oxygen were fed separately to the tube and shell sides respectively and they were allowed to react inside the catalytic membrane. In addition to methane combustion, partial oxidation and possibly water gas shift and steam reforming took place in palladium membrane since production of CO and H_2 was observed especially at high temperatures. Applying a pressure difference across the membrane improved performance of the reactor in terms of decreasing CO and H_2 concentrations but conversion increased only slightly. CO and H_2 were not observed for a Pd/α-Al_2O_3 membrane operated in dead-end mode. Platinum membranes showed lower CO production at high temperatures (beyond 580 °C) but H_2 was never detected in the outlet gases.

Acknowledgements

We gratefully acknowledge EPSRC for financial support and Buehler for providing the colloidal silica solutions.

References

[1] J. Coronas, M. Menendez, J. Santamaria, Development of ceramic membrane reactors with a non-uniform permeation pattern—application to methane oxidative coupling, Chem. Eng. Sci. 49 (24A) (1994) 4749–4757.

[2] J. Coronas, J. Santamaria, Catalytic reactors based on porous ceramic membranes, Catal. Today 51 (3) (1999) 377–389.

[3] C.F. Cullis, B.M. Willatt, Oxidation of methane over supported precious metal catalysts, J. Catal. 83 (1983) 267–285.

[4] T. Griffin, W. Weisenstein, V. Scherer, M. Fowles, Palladium-catalysed combustion of methane: simulated gas turbine combustion at atmospheric pressure, Combust. Flame 101 (1995) 81–90.

[5] R.E. Hayes, S. Kolaczkowski, Introduction to Catalytic Combustion, Gordon and Breach, Amsterdam, 1997.

[6] E. Kikuchi, Y. Chen, Syngas formation by partial oxidation of methane in palladium membrane reactor, in: Natural Gas Conversion V, vol. 119 of Studies in Surface Science and Catalysis, 1998, pp. 441–446.

[7] D. Lafarga, J. Santamaria, M. Menendez, Methane oxidative coupling using porous ceramic membrane reactors. 1. Reactor development, Chem. Eng. Sci. 49 (12) (1994) 2005–2013.

[8] J.H. Lee, D.L. Trimm, Catalytic combustion of methane, Fuel Process. Technol. 42 (2) (1995) 339–359.

[9] M. Murru, A. Prabowo, A. Gavriilidis, Preparation and characterisation of Pd and Pt/SiO_2–Al_2O_3 non-permselective membranes, J. Membr. Sci. (2003) in review.

[10] K. Muto, N. Katada, M. Niwa, Complete oxidation of methane on supported palladium catalyst: support effect, Appl. Catal. A: General 134 (2) (1996) 203–215.

[11] H.W.J.P. Neomagus, G. Saracco, H.F.W. Wessel, G.F. Versteeg, The catalytic combustion of natural gas in a membrane reactor with separate feed of reactants, Chem. Eng. J. 77 (3) (2000) 165–177.

[12] R. Prasad, L.A. Kennedy, E. Ruckenstein, Catalytic combustion, Catal. Rev.-Sci. Eng. 26 (1) (1984) 1–58.

[13] J.R. Rostrup-Nielsen, Catalytic steam reforming, in: J.R. Anderson, M. Boudart (Eds.), Catalysis Science and Technology, Springer-Verlag, Berlin, 1984.

[14] J.G. Sanchez Marcano, T.T. Tsotsis, Catalytic Membranes and Membrane Reactors, Wiley–VCH, Weinheim, 2002.

[15] G. Saracco, V. Specchia, Catalytic inorganic-membrane reactors—present experience and future opportunities, Catal. Rev.-Sci. Eng. 36 (2) (1994) 305–384.

[16] G. Saracco, J.W. Veldsink, G.F. Versteeg, W.P.M. van Swaaij, Catalytic combustion of propane in a membrane reactor with separate feed of reactants. I. Operation in absence of trans-membrane pressure-gradients, Chem. Eng. Sci. 50 (12) (1995) 2005–2015.

[17] G. Saracco, J.W. Veldsink, G.F. Versteeg, W.P.M. van Swaaij, Catalytic combustion of propane in a membrane reactor with separate feed of reactants. II. Operation in presence of trans-membrane pressure-gradients, Chem. Eng. Sci. 50 (17) (1995) 2833–2841.

[18] G. Saracco, J.W. Veldsink, G.F. Versteeg, W.P.M. van Swaaij, Catalytic combustion of propane in a membrane reactor with separate feed of reactants. III. Role of catalyst load on reactor performance, Chem. Eng. Commun. 147 (1996) 29–42.

[19] G. Saracco, H.W.J.P. Neomagus, G.F. Versteeg, W.P.M. van Swaaij, High-temperature membrane reactors: potential and problems, Chem. Eng. Sci. 54 (13) (1999) 1997–2017.

[20] G. Saracco, V. Specchia, Inorganic membrane reactors, in: A. Cybulski, J.A. Moulijn (Eds.), Structured Catalysts and Reactors, Marcel Dekker, New York, 1998, pp. 463–500.

[21] G. Saracco, V. Specchia, Catalytic combustion of propane in a membrane reactor with separate feed of reactants. IV. Transition from the kinetics to the transport-controlled regime, Chem. Eng. Sci. 55 (18) (2000) 3979–3989.

[22] H.J. Sloot, C.A. Smolders, W.P.M. van Swaaij, G.F. Versteeg, High-temperature membrane reactor for catalytic gas–solid reactions, AIChE J. 38 (6) (1992) 887–900.

[23] H.J. Sloot, G.F. Versteeg, W.P.M. van Swaaij, A nonpermselective membrane reactor for chemical processes normally requiring strict stoichiometric feed rates of reactants, Chem. Eng. Sci. 45 (8) (1990) 2415–2421.

[24] D.L. Trimm, C.W. Lam, The combustion of methane on platinum–alumina fibre catalysts. I. Kinetics and mechanism, Chem. Eng. Sci. 35 (1980) 1405–1413.

[25] D.L. Trimm, Catalytic combustion (Review), Appl. Catal. 7 (1983) 249–282.

[26] D.L. Trimm, Materials selection and design of high temperature catalytic combustion units, Catal. Today 26 (1995) 231–238.

[27] D.L. Trimm, Z.I. Önsan, Onboard fuel conversion for hydrogen-fuel-cell-driven vehicles, Catal. Rev.-Sci. Eng. 43 (1) (2001) 31–84.

[28] J.W. Veldsink, R.M.J. Vandamme, G.F. Versteeg, W.P.M. van Swaaij, A catalytically active membrane reactor for fast, exothermic, heterogeneously catalyzed-reactions, Chem. Eng. Sci. 47 (9) (1992) 2939–2944.

[29] D. Wolf, M. Hoehenberger, M. Baerns, External mass and heat transfer limitations of the partial oxidation of methane over Pt/MgO catalyst—consequences for adiabatic reactor operation, Ind. End. Chem. Res. 36 (1997) 3345–3353.

[30] Y.F. Yu Yao, Oxidation of alkanes over noble metal catalysts, Ind. Eng. Chem. Res. Dev. 19 (1980) 293–298.

[31] J. Zaman, A. Chakma, Inorganic membrane reactors, J. Membr. Sci. 92 (1) (1994) 1–28.

[32] M.F. Zwinkels, S.G. Järas, P. Govind Menon, Catalytic materials for high-temperature combustion, Catal. Rev.-Sci. Eng. 35 (3) (1993) 319–358.